Spermidine and Chloroquine Enhance Peptide-Based pDNA Transfection Efficiency within the GRP78-Overexpressing DU145 Prostate Cancer Cells

Grace Daniel
Carleton University
Filiz Collak
Carleton University
George Hilan
Carleton University
Elissa Robillard
Carleton University
William G. Willmore
Carleton University
Bruce C. McKay
Carleton University
David Sabatino
david.sabatino@carleton.ca

Carleton University

Research Article

Keywords: cancer-targeting peptides, GRP78, polyarginine, cell-penetrating peptides, chloroquine, spermidine, pDNA

Posted Date: October 17th, 2024

DOI: https://doi.org/10.21203/rs.3.rs-4966373/v1

Additional Declarations: No competing interests reported.

Abstract

This study describes a peptide-based formulation for plasmid gene (pDNA) delivery within the GRP78-overexpressing prostate cancer (DU145) cells. The GRP78-targeting sequence (WIFPWIQL) extended with the nona-arginine (R9) cell-penetrating peptide (WIFPWIQL-R9) effectively enabled capture and release of pDNA, while conferring serum stability, according to agarose gel electrophoresis. Characterization studies based on transmission electron microscopy revealed the formation of stably condensed peptide:pDNA nanoparticles (<200 nm) at excess peptide nitrogen (N) to pDNA phosphate (P) stoichiometric ratios (10:1 N/P) and with $CaCl_2$ functioning as an ionic stabilizer, that rendered the nanoparticles applicable to cell biology. Confocal imaging of the FITC-labeled peptide:pDNA formulation indicated cell uptake and intracellular entrapment within endosomes that restricted pDNA gene expression in the DU145 cells. Optimization studies with a reporter plasmid Green Fluorescent Protein (pGFP) revealed spermidine and chloroquine as the most effective additives for enhancing peptide-based transfection efficiency. Furthermore, blocking with anti-GRP78 confirmed the GRP78-dependent mechanism for cell uptake. Thus, peptide-targeting of GRP78 allows for selective binding and entry within the GRP78-overexpressing cancer cells for gene (pDNA) delivery. Transfection of the tumor suppressor p53-expression vector using the optimized peptide-based transfection conditions revealed elevated levels of p53 within the DU145 prostate cancer cells. These findings indicate the potential anti-cancer utility of the GRP78-targeting peptide gene (pDNA) delivery system.

Introduction

Peptides form an interesting class of small- to intermediate-sized biomolecules that can be readily synthesized by conventional solid-phase synthesis procedures (Coin et al. 2007).[1] Peptide modifications (peptidomimetics), including the incorporation of un-natural amino acids, cross-linking agents, spacers and linkers, as well as branching and cyclization motifs that also template supramolecular self-assembly have produced a vast array of synthetic peptide mimicry for investigating structure-activity relationships (Wynne et al. 2024).[2] Furthermore, synthetic peptides have been combined with various (bio)molecular (*e.g.*, nucleic acids, polysaccharides, lipids and proteins) probes and cargo (*e.g.*, fluorophores, quantum dots, nanoparticles, and radionuclides) that enables diagnostic visualization and homing capabilities with receptor and cellular targets (Ilies et al. 2024).[3] These include the cell-penetrating and cell-targeting peptides (CPPs and CTPs) functionalized with biomolecules, synthetic polymers and small molecule ligands that have been used for cell uptake and intracellular biological activity studies (Shah et al. 2020).[4] Arginine-rich CPPs have shown favorable cell translocation activities due to the cationic guanidinium side chain group of arginine that confers favorable electrostatic interactions with the negatively charged phospholipid membrane bilayer of cells (at physiological pH ~ 7). Cell permeability for arginine-rich cell-penetrating peptides occurs via a variety of cell uptake mechanisms. Arginine-rich CPPs can demonstrate sequence- (polyarginine length) and concentration-dependent cell uptake by membrane recognition, destabilization, pore formation and translocation into the cytosol of the cell (Herce et al. 2009).[5] The CPPs can also interact favorably with a variety of cell membrane-spanning

glycoprotein receptors (*e.g.*, heparan sulfate proteoglycans) that favor energy-dependent caveolae and clathrin-mediated endocytosis as well as macropinocytosis cell uptake pathways (Madani et al. 2011).[6] The inclusion of intracellular localization domains in cell-penetrating peptides, such as mitochondrial (MLS) and nuclear localization sequences (NLS), enables peptide intracellular localization into specific organelles (Xu et al. 2016 and Jean et al. 2016).[7,8] Considering the amphiphilic, polycationic nature of the CPPs, they can also favor stable electrostatic interactions with negatively charged nucleic acids (DNA and RNA), creating condensed ionic complexes suitable for the delivery of genetic therapies in cells, tissues and *in vivo* (Cardoso et al. 2013 and Lehto et al. 2011).[9,10] Of particular interest are the arginine-rich peptides that have been investigated for their ability to condense plasmid DNA (pDNA) into small, easy to transfect nanoparticles for gene expression. For example, the TAT (RKKRRQRRR) CPP formed a stable complex with pDNA, that effected cell-uptake and entry into the nucleus with a nuclear localization sequence (NLS, PKKKRKV) resulting in vascular endothelial growth factor (VEGF) expression and angiogenic effects in a hindlimb ischemia *in vivo* model (Qu et al. 2013).[11] A comparative study in between various arginine-rich CPPs, indicated that the TAT and polyarginine (R9), peptides improved cell uptake and expression of the Green Fluorescent Protein (GFP) reporter in the HEK-293 (a virus-immortalized kidney cell line) and HCC827 (a human lung cancer cell line) (Milech et al. 2015).[12] The introduction of non-polar/hydrophobic residues (Trp, His, and Ala), polymer scaffolds, peptide stapling, branching and cyclization from medium-to-large-sized macrocycles produce modified arginine-rich peptides with enhanced cell uptake, endosomal escape and gene expression capacity (Szabo et al. 2002).[13] Despite their cell-based and *in vivo* activities, the arginine-rich CPPs remain non-specific gene delivery agents, thereby limiting efficacy and raising toxicity concerns in therapeutic applications (Zhang et al. 2015).[14]

The CTPs function as an important class of cancer-targeting agents, that selectively bind to cancer cell surface receptors for specific detection and treatment of tumors (Zhang et al. 2023).[15] A variety of selection methods, such as phage display biopanning, combinatorial library and parallel (micro)array peptide screening, as well as *in silico* molecular modeling and docking studies have led to the discovery of novel CTPs against key receptor and cellular cancer targets (Todaro et al. 2023 and Liu et al. 2017).[16,17] The CTPs have been conjugated with a variety of imaging and therapeutic agents for cancer-targeted therapy (Yang et al. 2022).[18] Of specific interest to this study, the W peptide sequence, WIFPWIQL, is a GRP78-targeting peptide capable of binding to cell surface Glucose Regulated Protein 78 (csGRP78), an endoplasmic reticulum stress-inducible chaperone protein that is overexpressed and translocated to surface of a variety of cancer cell lines, but is absent or minimally presented on the surface of non-malignant cell types (Arap et al. 2004).[19] The W-peptide selected by phage display biopanning to target csGRP78 on prostate and breast tumor tissues (Arap et al. 2004),[19] demonstrates specific GRP78 binding and not to other related, homologous chaperones (*e.g.*, heat shock proteins 70, Hsp70, and 90, Hsp90), moderate dose (50 μM) binding activity with rapid association/dissociation kinetics (k_{on}/k_{off}) according to surface plasmon resonance (Wang et al. 2016),[20] at the peptide binding domain of GRP78, based on molecular modeling and docking studies (Wang et al. 2016 and 2018).[21,22]

The W-peptide also displayed GRP78-specific binding on the surface of prostate (DU145) cancer cells, with decreased binding detected in competition with soluble GRP78 and a blocking polyclonal anti-GRP78 (Arap et al. 2004).[19] Accumulation of the W-peptide was also observed in the DU145 cells and at the localized tumor site within mice xenograft models, with notable regression in tumor growth upon administration of the chimeric W-peptide and the pro-apoptotic (D-(KLAKLAK)$_2$) sequence (Arap et al. 2004).[19] Despite its *in vitro* and *in vivo* anti-cancer activities, the GRP78-targeting W-peptide retains poor cell uptake efficiency and is unable to deliver gene therapeutics directly into cancer cells.

To address this limitation, this work reveals that the addition of the CPP sequence, R9, to the GRP78-targeting W-peptide, produces a novel polyarginine-derived GRP78-targeting peptide sequence (FITC-Ahx-WIFPWIQL-GG-R9-GG, Fig. 1A). Peptide synthesis and characterization have been reported in our previous study (Daniel et al. 2024).[23] This peptide is also conjugated to the fluorochrome fluorescein isothiocyanate (FITC), linked to an aminohexanoic acid (Ahx) linker at the *N*-terminus for imaging cell binding and permeability of the peptide in combination with pDNA expression vectors. The incorporation of Gly (-GG-) spacers in between the CTP (W-peptide) and CPP (R9) domains and at the peptide *C*-terminus provides spatial distance in between each peptide functional domain that enables gene delivery directly within csGRP78-presenting DU145 prostate cancer cells (Fig. 1B). Formulation studies of the peptide:pDNA (nano)particles examined the influence of stoichiometry (peptide nitrogen to pDNA phosphorus (N:P) ratios), annealing buffer and serum stability in media, as well as the role of additives (*e.g.*, $CaCl_2$, heparin, spermidine and chloroquine, among others) on the formation of stably condensed, and reversible peptide:pDNA ionic complexes, that function as dynamic capture and release gene delivery systems. This characterization study using mock (pUC19 and pBR32) and reporter (pGFP) plasmid (pDNA) expression vectors led to the discovery of an optimized peptide-based transfection protocol. Peptide-based transfections of the wild-type p53 tumor suppressor expression vector within the GRP78-presenting DU145 prostate cancer cells indicated noticeable p53 induction, underscoring their promising anti-cancer utility.

Results and Discussion

Formulation of Peptide:pDNA Nanoparticles

The optimization of the peptide:pDNA formulation was initially based on screening the favorable stoichiometry of the polycationic peptide nitrogen to the polyanionic pDNA phosphorous (1:1-20:1, N:P) mole ratios that promotes stable peptide:pDNA ionic complex formation in annealing (50 mM Tris-HCl and 150 mM NaCl, pH 7.5) buffer. An agarose gel-shift electrophoretic mobility assay in between peptide (polyarginine CPP, R9, *vs.* CTP-CPP, W-R9) and the pUC19 (2,686 base-pair) pDNA vector, revealed complete disappearance of the pDNA band alone and formation of a more retained complex with excess (10-20:1) N:P peptide:pDNA ratios that effectively form stable ionic complexes (Fig. 2A). This provides a binary approach for confirming the ideal N:P stoichiometric ratio in buffer, by demonstrating formation of the more retained, higher-order peptide:pDNA ionic complex that also excludes external dye (ethidium

bromide) binding and staining of the pDNA vector. A similar outcome was observed with the FITC-labeled R9 peptide and the larger (4,361 base-pairs) pBR322 pDNA, that also suggests samples in unbound (FITC-R9) *vs*. bound (FITC-R9:pDNA) states, highlighting the versatility of the peptides to form stable complexes with various-sized vectors (Fig. 2B). Interestingly, these results also show that the hydrophilic, polycationic R9 CPP can effectively form stable ionic complexes with pUC19 at a 1:1 N:P ratio, presumably due to the unimpeded electrostatic interactions, while the amphiphilic W-R9 CTP-CPP requires a 10:1 N:P ratio to form the stable peptide:pDNA complex (Fig. 2A). The hydrophobic GRP78-targeting W peptide sequence may hinder the formation of stable peptide:pDNA ionic complexes at stoichiometric equivalence. However, this limitation is overcome with excess peptide:pDNA N:P ratios, while the amphiphilic nature of the W-R9 peptide may also enable more favorable csGRP78 receptor and membrane interactions for gene delivery (Lozanda et al. 2023 and Alkhamy et al. 2016).[24,25]

An optimal N:P stoichiometric ratio is thus essential for achieving efficient peptide condensation of pDNA, while maintaining peptide:pDNA ionic complex stability that may also ensure protection against enzymatic degradation that prolongs transfection efficiency. The stability of the peptide:pDNA complex was next investigated against enzymes such as nucleases or proteases present within serum containing media used in cell culture transfection conditions (Adami et al. 1998).[26] The peptide:pDNA samples were incubated in Eagle's Minimal Essential Medium (EMEM) containing 10% fetal bovine serum (FBS), and aliquots at various time points (1-24 h.) were collected and analyzed on agarose gel electrophoresis (Fig. 2C). The stability of pUC19 in FBS:EMEM at short (1 h.) and extended (24 h.) incubation times indicated some changes in the integrity of the pDNA band, by the appearance of more-retained, smear of bands with slower electrophoretic mobility on gel *vs.* pUC19 alone (Fig. 2C). This may be an indication of nick(s) in the pDNA resulting in the formation of linear, knotted or catenated DNA structures that transitions circular into open-chained DNA with slower electrophoretic mobility compared to the unnicked condensed circular pDNA vector (Cebrian et al. 2015).[27] This outcome confirms that the pDNA is unstable in the FBS-containing media conditions. In contrast, the peptide:pDNA complex (W-R9:pUC19) shows good stability in FBS:EMEM throughout the entire 24 hour incubation period (Fig. 2C). This sample displayed only very faint, slower moving pDNA bands, with no visible changes in intensities over the 24-hour incubation period in FBS:EMEM. The faint bands may be due to minimal quantities of unbound pDNA, that were absent of stable ionic complex with peptide and enzyme exposed for degradation. However, the W-R9 peptide sufficiently forms stable ionic complex with pDNA and provides substantial protection from enzymatic digestion in serum-containing media during the 24-hour incubation period, thereby bolstering its potential transfection utility.

Heparin is a polyanionic sulfated glycosaminoglycan polysaccharide that is commonly used in displacement assays to confirm the reversible capture-release nature of non-covalent, ionic complexes (Ryu et al. 2011).[28] In this assay (Fig. 2D), heparin sodium salt was added to outcompete the binding capacity of the cationic peptide (W-R9 and R9) for the anionic pDNA (pUC19), thereby releasing the pDNA vector in its free form. The heparin displacement assay validates the reversibility of the peptide:pDNA ionic complex, that is applicable to the capture and release of pDNA for gene expression.

Heparin competitive binding displacement of the pUC19 pDNA vector from the peptides, W-R9 (Fig. 2D) and R9 (Fig. S1, ESI), in a dose-dependent (1-10 mg) manner, was confirmed by the reappearance of the pDNA band upon heparin addition, when compared to the peptide:pDNA ionic complex (10:1 N:P ratio) without heparin. The fainter pUC19 band intensities with lower-dose (1 µg) compared to higher-doses (2.5-10 µg) of heparin indicates that some peptide remains bound to the pUC19 at lower heparin treatment conditions, and with complete displacement of pDNA with increased addition of heparin. This result aligns with literature precedence, showing the ability of heparin to displace peptides from pDNA vectors (Ryu et al. 2011).[28] Overall, this result indicates that W-R9 forms a reversible ionic complex with a pUC19 pDNA, that effectively functions as a capture and release system for gene delivery.

Transmission electron microscopy (TEM) imaging (Fig. 3) of the peptide:pDNA ionic complexes (FITC-W-R9 combined with pUC19 at a 10:1 N:P ratio in milliQ H_2O) was next conducted to gain a visual representation of the relative sizes and shapes of the (nano)particles with (Fig. 3B) and without (Fig. 3A) $CaCl_2$, functioning as ionic stabilizer (Alkhamy et al. 2016 and Baoum et al. 2012).[25,29] The peptide:pDNA complex alone shows a disordered aggregated assembly of large particles, whereas $CaCl_2$ condensed the peptide:pDNA ionic complex into smaller (< 200 nm), discrete nanoparticles that may be applicable to gene delivery. In the absence of $CaCl_2$, the peptide:pDNA complex appears to form larger aggregated structures, that may impede cell uptake and reduce gene delivery efficacy (Cultrara et al. 2019).[30] Therefore, the ability to condense stable and reversible peptide:pDNA ionic complexes into small, discrete and uniform nanoparticles is another important requirement for effective gene delivery (Su et al. 2022).[31] Various conditions exist for condensing pDNA-based ionic complexes, including $CaCl_2$, that also improves cell uptake efficiency when used in combination with cell penetrating peptides (Su et al. 2022, Alkhamy et al. 2016 and Baoum et al. 2012).[25,29,31] Furthermore, $CaCl_2$ has also been reported to enhance the endosomal escape capacity of nucleic acid cargo resulting in enhanced transfection efficacy (Khondee et al. 2011).[32] Mechanistic studies revealed the combined Ca^{2+} effects on the peptide:pDNA ionic complex that promotes membrane destabilization and pore formation for enhancing cell uptake, while also promoting endosomal rupture and release of pDNA for gene expression (Alkhamy et al. 2016).[25] Thus, $CaCl_2$ has been effectively shown to condense the peptide:pDNA ionic complexes into stable nanoparticles that improves transfection efficiency.

Cell Biology of Peptide:pDNA Nanoparticles

A preliminary cell uptake study was conducted to test the transfection capabilities of the fluorescein-labeled polyarginine-derived GRP78-targeting peptide (FITC-W-R9) in combination with a mock pBR322 vector within the DU145 prostate cancer cells (Fig. 4). Confocal fluorescence microscopy was used to confirm cell uptake and determine the subcellular localization of the polyarginine-derived GRP78-targeting peptide:pDNA (FITC-W-R9:pBR322). Punctate areas of green fluorescence (green arrows, Fig. 4) were detected in the cytosol of transfected DU145 cells. This observation suggests the entrapment of the peptide-based pDNA formulation in vesicle-type endosomes may restrict pDNA release for gene

expression. This result also aligns with the reported clathrin-receptor mediated endocytosis cell uptake mechanism of GRP78-targeting peptides (Kim et al. 2006 and Liu et al. 2007).[33,34] This pathway has been associated with the active peptide-binding and ATPase domains of csGRP78, that favor formation of clathrin-coated pits that detach from the plasma membrane to form intracellular vesicles via receptor-mediated endocytosis of peptide ligands (Liu et al. 2007).[34] Although polyarginine-derived GRP78-targeting peptides can improve cell uptake (Joseph et al. 2014),[35] intracellular entrapment may restrict its drug (gene) delivery efficacy.

Transfection efficiency was initially tested with a reporter Green Fluorescent Protein (GFP)-expressing pDNA (pGFP) in combination with the polyarginine-derived GRP78-targeting peptide (W-R9) that formed the peptide:pDNA (W-R9:pGFP) nanoparticles. A direct comparison of the peptide-based (W-R9) pGFP transfection efficiency with the benchmark Lipofectamine™ 3000 cationic lipid transfection agent indicated poor (<5%) GFP expression signaling with the peptide:pDNA conditions (Fig. 5B), whereas Lipofectamine™ 3000 effected noticeable (25-35%) GFP detection (Fig. 5A) according to fluorescence microscopy (Fig. S2, ESI). The insignificant peptide-based pDNA transfection efficiency may be due to the large, aggregated particles apparent by TEM imaging (Fig. 3A), that inhibits cell uptake (Cutrara et al. 2019),[30] or incomplete endolysosomal escape, that is consistent with the punctate fluorescent (FITC) nanoparticles suggestive of peptide;pDNA entrapment within vesicle-type endosomes in the DU145 cells (Fig. 4).

A variety of additives, commonly used to improve peptide:pDNA transfection efficiency (Baoum et al. 2012, Ibanez et al. 1996, Yang et al. 2009, Griesenbach et al. 2012 and Alhakamy et al. 2013 and 2016),[25,29,36-39] were screened and selected to optimize the peptide-based (W-R9) transfection conditions with the reporter pGFP vector within the DU145 cells. For example, $CaCl_2$ was added to condense the peptide:pDNA formulation into stable nanoparticles via favourable electrostatic interactions (Fig. 3B), that was also anticipated to enhance cell uptake (Alhakamy et al. 2016 and Baoum et al. 2012).[25,29] Moreover, $CaCl_2$ has been used to increase endosomal escape of cationic cell-penetrating peptides and pDNA nanoparticles (Alhakamy et al. 2013).[39] The addition of $CaCl_2$ (50, 150, and 300 mM) exhibited modest effects on the peptide-based pGFP transfection, and resulted in apparent toxicity to the DU145 cells, especially at higher concentrations (300 mM) and extended (48-72 h.) incubations (Fig. S3, ESI). Trans-cyclohexane-1,2-diol (TCHD) was also tested for its ability to increase peptide-based transfection efficiency with the pGFP reporter. TCHD has been shown to enlarge the nuclear pores, thereby collapsing the permeability barrier across the nuclear membrane, for nuclear uptake of larger biomacromolecules, including pDNA for gene expression (Griesenbach et al. 2012).[38] The addition of TCHD (0.5, 1.0, 2.0 %) also moderately improved the peptide-based pGFP transfection efficiency according to fluorescence microscopy, while producing significant toxicity to the DU145 cells, even at low doses (Fig. S4, ESI). Due to cell toxicity, $CaCl_2$ and TCHD were discontinued in the optimization of peptide-based pDNA transfection studies.

Spermidine and chloroquine were next evaluated to optimize the peptide-based transfection conditions with the reporter pGFP in the GRP78-presenting DU145 cells (Wong-Baeza et al. 2010).[40] Spermidine is a polycationic polyamine that aides in the condensation of nucleic acids and favors the intracellular release of pDNA for gene expression (Ibanez et al. 1996).[36] Chloroquine, functions as a lysosomotropic agent that increases the lysosomal pH, thereby directly disrupting endosomal membranes contributing to endolysosomal escape of cargo for intracellular activity (Yang et al. 2009).[37] Transfection studies have used chloroquine and spermidine in combination with liposomal-based gene delivery agents, that served to improve transfection efficiency resulting in enhanced gene expression (Moradpour et al. 1996 and Zhang et al. 2023).[41,42] In this study, the peptide-based (W-R9) transfection efficiency of pGFP was examined in the presence and absence of chloroquine and spermidine, and compared to the benchmark Lipofectamine 3000 transfection reagent (Fig. 5). The combination of chloroquine and spermidine (70 and 17.5 μM, respectively) improved the transfection efficiency of the peptide:pDNA complex, resulting in enhanced pGFP expression (Fig. 5C) compared to the peptide:pDNA transfection conditions that were absent of the additives and displayed very little, faint fluorescence signaling (Fig. 5B). Chloroquine and spermidine also maintained good cell viability compared to the previously tested peptide-based pGFP transfection conditions (Figs. S3 and S4, ESI). In comparison, the pGFP transfection conditions with chloroquine and spermidine, but absent of peptide, displayed background GFP fluorescence, as negative control (Fig. 5D). Alternatively, the Lipofectamine:pGFP transfection condition promoted GFP expression, as positive control (Fig 5A). This outcome demonstrates the ability for the select additives, chloroquine and spermidine, to improve the peptide:pDNA transfection efficiency, while maintaining cell viability at low effective concentrations underscoring their utility as safe and effective additives for promoting peptide-based gene delivery.

The optimized peptide-based (W-R9) pGFP transfection conditions with chloroquine and spermidine were also used to confirm the GRP78-dependent mechanism of cell uptake resulting in GFP expression (Fig. 6). In competition with the primary GRP78/Bip monoclonal antibody (1D6F7), selected to block the peptide-binding domain (351-654) of csGRP78, the pGFP expression was diminished in the peptide-based transfection with chloroquine and spermidine (Fig. 6B). In comparison, the peptide-based transfection conditions with chloroquine and spermidine, in the absence of anti-GRP78 displayed an increase in GFP signaling (Fig. 6A). Alternatively, the negative control pGFP transfection conditions with chloroquine and spermidine alone, produced negligible GFP signaling (Fig. 6C). Significantly, this result provides direct evidence of the GRP78-dependent peptide:pDNA cell uptake mechanism that results in pGFP expression within the DU145 cells (Fig. 6A *vs.* 6B). Therefore, the GRP78-targeting polyarginine peptide (W-R9) functions as a gene delivery system within csGRP78-presenting tumors for applications in the cancer-targeted delivery of gene (pDNA) therapeutics.

The translational, anti-cancer utility of the optimized peptide-based transfection conditions was subsequently examined with a plasmid vector applicable to cancer-targeted gene therapy. The p53 pDNA expression vector was used to produce wild-type tumor suppressor protein p53 within the representative DU145 prostate cancer (PCa) cell line expressing the csGRP78 biomarker (Arap et al. 2004)[19] and

mutant tumor tp53 oncogene (Chappell et al. 2012).[43] The tumor suppressor protein, p53, is long-regarded as the guardian of the human genome, acting as a critical transcription factor of multiple (~500) gene targets, including those involved in DNA repair, cell cycle arrest, senescence and apoptosis in transformed cancer cells (Lane 1992).[44] However, the anti-tumor activity of p53 is abolished in about half of all cancers due to excessive mutations and oncogenic tumor p53 signaling driving cancer cell proliferation, spread and therapy resistance (Muller et al. 2014).[45] Therefore, an effective gene therapy strategy will activate wild-type (wtp53) gene expression to restore tumor suppression, resulting in potent anti-cancer responses (Chappell et al. 2012 and Yu et al. 2004).[43,46] The optimized peptide-based (W-R9) pDNA transfection conditions with chloroquine and spermidine were used in a preliminary study, to express the wild-type p53 tumor suppressor within the DU145 PCa cells, known to express mutant tp53 variants (Chappell et al. 2012).[43] Western blot indicated the protein expression levels of the wild-type p53 isoforms, detected significantly with the control Lipofectamine™ 3000 transfection agent (Fig. 7, lane 2), and to a lesser, but noticeable extent with the optimized peptide-based transfection conditions (Fig. 7, lane 4). Interestingly, the peptide-based transfection conditions in the absence of the additives, chloroquine and spermidine, did not produce detectable levels of p53 (Fig. 7, lane 3), that was consistent with the poor pGFP transfection efficiency observed for the W-R9 peptide alone (Fig. 5B). However, in combination with chloroquine and spermidine additives, an enhancement in peptide-based transfection efficiency is observed (Figs., 5C, 6A and 7, lane 4). Alternatively, that additives chloroquine and spermidine in the absence of peptide (W-R9) do not enable protein expression (Figs., 5D, 6C and 7, lane 5). Therefore, the polyarginine-derived GRP78-targeting peptide (W-R9), with chloroquine and spermidine additives, enhances gene (pDNA) delivery directly within the GRP78-overexpressing DU145 prostate cancer cells. These exploratory results also suggest the ability to restore the functional, anti-tumor responses of the wild-type p53 tumor suppressor directly within the DU145 cells, and to overcome the oncogenic effects of mutant (tp53) biomarkers, leading towards the innovation of a promising cancer-targeted gene therapy approach.

Conclusions

This study describes the gene delivery applications of an optimized formulation of peptide:pDNA nanoparticles for cell-based detection and treatment in the GRP78-overexpressing DU145 prostate cancer cells. A nona-arginine (R9) cell penetrating peptide was added to the GRP78-targeting peptide sequence (WIFPWIQL) to produce the (WIFPWIQL-R9) chimeric peptide that effectively formed stable pDNA ionic complexes in annealing buffer conditions. Characterization data confirmed formation of stably condensed peptide:pDNA nanoparticles (< 200 nm), at excess peptide nitrogen (N) to pDNA phosphate (P) stoichiometric ratios (10:1 N/P) and with $CaCl_2$ functioning as ionic stabilizer, thereby rendering the nanoparticles applicable to cancer cell biology. Confocal imaging of the FITC-labeled peptide:pDNA formulation indicated cell uptake and intracellular localization within endosomes that restricted gene expression in the DU145 cells. Optimization studies with the peptide:pGFP reporter system investigated the effects of additives ($CaCl_2$, spermidine and chloroquine, among others) on transfection efficiency as a function of gene (GFP) expression. This screen revealed the combined,

synergistic effects of additives (chloroquine and spermidine) resulting in an enhancement in the peptide:pDNA transfection efficiency. The application of anti-GRP78 also validated the GRP78-dependent cell uptake mechanism of the peptide:pGFP formulation. Preliminary investigations into the peptide-based transfection of the wild-type p53 vector in the GRP78-presenting DU145 prostate cancer cells produced noticeable expression of the p53 tumor suppressor. Significantly, the optimization of a peptide-based transfection protocol may be broadly applicable to a variety of gene therapeutics, for gene delivery selectively within csGRP78-presenting tumors, leading to the innovation of an impactful cancer-targeted gene therapy approach.

Materials and Methods

Peptide synthesis and characterization

All peptides were designed synthesized and characterized following the recently published procedures (Daniel et. al. 2024).[23]

Stoichiometric peptide nitrogen to nucleic acid phosphorus (N:P) ratios

In order to determine the optimal peptide nitrogen (N) to pDNA phosphate (P) stoichiometric ratios, the samples were prepared at various N:P ratios; 1:1, 10:1, and 20:1 following a literature protocol (Aydin et al. 2022).[47] Peptide (FITC-R9, R9 and W-R9, 3.06×10^{-10} - 6.15×10^{-9} mol) and pDNA (pUC19 and pBr322, 3.06×10^{-10} mol) combinations were incubated in Tris buffer (50 mM Tris-HCl and 150 mM NaCl, pH 7.5) and diluted in dH_2O to a set volume (24 µL). All samples were incubated for 30 min. at room temperature. A sample of only pDNA was also prepared as control.

Dye exclusion agarose gel electrophoresis

A 1% non-denaturing agarose gel was prepared for 30 minutes. A tracking dye (6X TrackIt Cyan/Orange loading buffer, ThermoFisher cat. no. 10488085) was added to each peptide:pDNA sample. The peptide:pDNA test samples, along with pDNA alone and a base pair ladder (TrackIt 1Kb Plus DNA Ladder, ThermoFisher cat. no. 10488085) were added to the agarose gel. The gel was run in 1x TEA gel running buffer for 1 h. at 71 V. The gel was stained using ethidium bromide (EtBr) on a shaker for 1 hour and destained using dH_2O on a shaker at room temperature for 20 min. Gels were imaged using a Bio-Rad molecular imager and analyzed using ImageJ software.

Heparin release assay

Peptide:pDNA samples were prepared at a 10:1 N:P ratio using W-R9 peptide and pUC19 pDNA. Prior to adding the heparin, peptide:pDNA samples were incubated Tris buffer (50 mM Tris-HCl and 150 mM NaCl, pH 7.5) for 30 min. at room temperature. Heparin (1-10 µg) was prepared in Tris buffer (10 µL) then added to each peptide:pDNA sample in increasing quantities (1 µg, 2.5 µg, 5 µg, 7.5 µg, and 10 µg). Samples were incubated for 30 min. at room temperature and then diluted to volume (25 µL) using Tris

buffer. Agarose gel (1%, non-denaturing) electrophoresis was run and analyzed following the procedure previously described.

Fetal bovine serum (FBS) stability

Peptide:pDNA samples were prepared at a 10:1 N:P ratio using W-R9 peptide and pUC19 pDNA. Prior to addition of FBS, peptide:pDNA samples were incubated in Tris buffer (50 mM Tris-HCl and 150 mM NaCl, pH 7.5) for 30 min. at room temperature. An aliquot (20 µL) of 20 % FBS in Eagle's Minimum Essential Medium (EMEM) was added so each sample has a final concentration of 10% FBS in EMEM. A control peptide:pDNA sample was prepared in Tris buffer, absent of FBS in EMEM. Samples with FBS were left to incubate for 1, 2, 4, 6, and 24 hrs. at 37 ^{o}C. Samples of only pUC19 and FBS were prepared to a final concentration of 10% FBS and collected at 1 h and 24 hrs. The samples were centrifuged, separated, quenched with gel loading buffer (6X TrackIt Cyan/Orange loading buffer), and frozen until being resolved on an agarose gel (1%, non-denaturing) electrophoresis following the procedure previously described.

TEM imaging

Peptide:pDNA samples were prepared at a 10:1 N:P ratio in milliQ H_2O. Samples were also incubated with 50 mM $CaCl_2$ (5 µL) for 30 min at room temperature. An additional aliquot (7.5 µL) of 1% uranyl acetate in milliQ H_2O was added to the samples to ensure equivalent volumes. Aliquots (10 µL) of individual samples were then deposited onto a 300-mesh formvar copper grid coated with carbon (Electron Microscopy Sciences Inc., Hatfield, PA). It was allowed to evaporate for 1 h. and TEM images were obtained using the FEI Tecnai G2 F20 Transmission Electron Microscope at an accelerating voltage of 120 kV and the Gatan ORIUS TEM CCD Camera was used to capture images across the grids. The Oxford X-Max 80 mm^2 Energy Dispersive X-ray (EDX) detector was used alongside Aztec software for EDX analysis. Particle size measurements of width, length, and diameter were taken using ImageJ software (LOCI, University of Wisconsin).

Cell culture

The prostate cancer mammalian cell line (DU145 cells) was gratefully obtained as a gift from Dr. Bruce McKay (Department of Biology, Carleton University). The culture conditions used MultiCell's Essential Modified Eagle's Medium (EMEM, 320-005-CL) supplemented with 10% heat inactivated fetal bovine serum (FBS) and incubated at 37˚C, in a ThermoForma triple gas (N_2-O_2-CO_2) incubator at 21% O_2 and 5% CO_2, with 95% relative humidity. All cell work was conducted in a biosafety cabinet (ThermoScientific – 1300 Series A2 Hood).

Fluorescence microscopy

For cell uptake studies, the DU145 cells, counted and seeded at a density of 3.5 x 10^5 cells per 35 cm plate for 24 hours, were incubated with the FITC-labeled peptide (W-R9) and pBR322 (10:1 N/P ratio in

Tris buffer) for 24 hours. The cells were washed twice with 1X PBS then fixed with 4% paraformaldehyde for 15 minutes, then washed again with 1X PBS twice. DAPI and Mito-Tracker were used to stain the cells. The coverslip was then inverted onto a 1.5 mm microscope slide and imaged on a Zeiss LSM 980 confocal microscope using the 63X magnification oil lens.

Cells were seeded to in a 24-well plate to 50,000 cells/well 24 hours prior to transfection optimization studies. Varying concentrations of TCHD (0.5, 1.0, 2.0 %), spermidine (7.5, 12.5, 17.5 μM), and $CaCl_2$ (50, 150, 300 mM) were added to separate 10:1 N:P aliquots of FITC-W-R9 and pcDNA3.1-GFP and incubated for one hour at room temperature in annealing Tris buffer. The media was changed to Opti-MEM (31985-070, Gibco), and the peptide:pGFP formulation was added dropwise to the wells. Lipofectamine transfection of pGFP was carried out according to the manufacturer's instructions (Thermo Fisher) and the media was replaced 4 hours post-transfection. Fluorescent images were taken 24 and 48 hours after transfection on the EVOS Fluorescence microscope (Thermo Fisher).

Transfection conditions

Cells were seeded in a 6-well plate to 250,000-350,000 cells/well 24 hours prior to transfection. The FITC-W-R9 peptide was combined with the pcDNA3.1-GFP or the pRc-cmv-p53 pDNA vector in a 10:1 M:P ratio, followed by the addition of 70 μM chloroquine (C6628, Sigma), 17.5 μM of spermidine (204-689-0, Sigma), in Tris buffer (50 μL). The solution was incubated at room temperature for 1 hour in the dark. The media was changed to Opti-MEM (31985-070, Gibco), and the peptide:pDNA formulation was added dropwise to the wells. Lipofectamine-based transfections were carried out according to the manufacturer's instructions (Thermo Fisher) and replaced to MultiCell's Essential Modified Eagle's Medium (EMEM, 320-005-CL) supplemented with 10% heat inactivated fetal bovine serum (FBS) 4 hours post-transfection. Fluorescent images for detection of GFP expression were taken 24 and 48 hours after transfection on the EVOS Fluorescence microscope (Thermo Fisher).

Western blot

Following transfection (48 h.), the DU145 cells were collected and pelleted in phosphate buffered saline (PBS) at 1,200 RPM for 5 mins and then lysed with RIPA buffer (89901, Thermofisher) for 20 mins on ice while gently shaking. The cell lysates were centrifuged at 12,000 RPM for 20 mins. The protein concentration from the supernatant was determined by Bradford assay (Bio-Rad). A 12% sodium dodecyl sulfate-polyacrylamide gel electrophoresis (SDS-PAGE) was prepared, with samples loaded with protein aliquots (20 μg). The gel was run at 120V for roughly 1.5 hours. Gel transfer on a PVDF membrane was completed with transfer buffer at 4˚C in the fridge and run overnight at 0.18 amps. The following day, the membrane was removed from the assembly, placed in a container, and blocked with 5% dry milk in 1X Tris-buffered saline-Tween 20 (TBST) for 1 hour in the fridge while shaking. After blocking, incubation with primary antibodies for probing p53 (sc-6243), PUMA (PC686, Calbiochem), p21 (OP64, EMD), and beta-actin (A5316, Sigma), were used at 1:1000 concentration 1X TBST at 4˚C overnight. The following day, the primary antibodies were collected for future use, and the membranes were washed for 25 minutes, five times with 1X TBST over a shaker at 4˚C. A secondary antibody conjugated with HRP was

then added to the corresponding membrane, at 1:5000 concentration in 1X TBST at 4˚C for 1 hour. The secondary antibodies were collected, and the membranes were washed for 25 minutes, five times with 1X TBST. To visualize the membranes, a Clarity Western ECL Substrate (#1705061, Bio-Rad) was added to the membranes and allowed to sit at room temperature in the dark for 5 minutes. After which, the chemiluminescence solution was removed and the membrane was placed in a plastic sheet and imaged on the Bio-Rad ChemiDoc station to visualise the proteins. ImageLab software was used for further analysis of all Western Blots including protein band densitometry to determine equal protein loading using beta-actin relative to treatment conditions.

Declarations

Acknowledgements

This work was gratefully supported by the Natural Sciences and Engineering Council Discovery Grant to D.S. (RGPIN-2024-05349) and W.G.W. (RGPIN-2017-06414) and the Canada Foundation for Innovation John R. Evans Leaders Fund and the Ontario Research Small Infrastructure Fund to D.S. (43604). The co-authors are also grateful to Dr. Jianqun Wang from the Carleton Nano Imaging Facility for assistance with TEM and EDX analysis of peptide:pDNA samples.

Author contributions

G.D., F.C., G.H. and E.R. conducted experimental investigations. W.G.W., B.C.M. and D.S., supervised and secured project funding, compiled and revised manuscript. All authors have read and approve this manuscript.

Statements and Declarations

The authors declare no conflicts of interest.

Supplementary Information†

The online version contains supplemental material available at:

Data Availability

No datasets were generated or analyzed in this study.

References

1. Coin I, Beyermann M, Bienert M. (2007) Solid-phase peptide synthesis: from standard procedures to the synthesis of difficult sequences. *Nat Protoc.*, 2:3247-3256. https://doi.org/10.1038/nprot.2007.454

2. Wynne C, Elmes BPR. (2024) Modified Synthetic Peptides: From Therapeutics to Chemosensors. *Sens Diagn.* **2024**, 3:987–1013. https://doi.org/10.1039/D4SD00022F
3. Ilieş BD, Yildiz I, Abbas M. (2024) Peptide-conjugated Nanoparticle Platforms for Targeted Delivery, Imaging, and Biosensing Applications. *Chembiochem*. 25:e202300867. https://doi.org/10.1002/cbic.202300867
4. Shah SS, Casanova N, Antuono G, Sabatino D. (2020) Polyamide Backbone Modified Cell Targeting and Penetrating Peptides in Cancer Detection and Treatment. *Front Chem*. 8:218. https://doi.org/10.3389/fchem.2020.00218
5. Herce HD, Garcia AE, Litt J, et al. (2009) Arginine-rich peptides destabilize the plasma membrane, consistent with a pore formation translocation mechanism of cell-penetrating peptides. *Biophys J*. 97:1917-1925. https://doi.org/10.1016/j.bpj.2009.05.066
6. Madani F, Lindberg S, Langel U, Futaki S, Gräslund A. (2011) Mechanisms of cellular uptake of cell-penetrating peptides. *J Biophys*. 2011:414729. https://doi.org/10.1155/2011/414729
7. Xu Y, Liang W, Qiu Y, et al. (2016) Incorporation of a Nuclear Localization Signal in pH Responsive LAH4-L1 Peptide Enhances Transfection and Nuclear Uptake of Plasmid DNA. *Mol Pharm*. 13:3141-3152. https://doi.org/10.1021/acs.molpharmaceut.6b00338
8. Jean SR, Ahmed M, Lei EK, Wisnovsky SP, Kelley SO. (2016) Peptide-Mediated Delivery of Chemical Probes and Therapeutics to Mitochondria. *Acc Chem Res*. 49:1893-1902. https://doi.org/10.1021/acs.accounts.6b00277
9. Cardoso AM, Trabulo S, Cardoso AL, et al. (2013) Comparison of the efficiency of complexes based on S4(13)-PV cell-penetrating peptides in plasmid DNA and siRNA delivery. *Mol Pharm*. 10:2653-2666. https://doi.org/10.1021/mp400078h
10. Lehto T, Simonson OE, Mäger I, et al. (2011) A peptide-based vector for efficient gene transfer in vitro and in vivo. *Mol Ther*. 19:1457-1467. https://doi.org/10.1038/mt.2011.10
11. Qu W, Qin SY, Ren S, Jiang XJ, Zhuo RX, Zhang XZ. (2013) Peptide-based vector of VEGF plasmid for efficient gene delivery in vitro and vessel formation in vivo. *Bioconjug Chem*. 24:960-967. https://doi.org/10.1021/bc300677n
12. Milech N, Longville BA, Cunningham PT, Scobie MN, et al. (2015) GFP-complementation assay to detect functional CPP and protein delivery into living cells. Sci Rep. 5:18329. https://doi.org/10.1038/srep18329
13. Szabó I, Yousef M, Soltész D, Bató C, Mező G, Bánóczi Z. (2002) Redesigning of Cell-Penetrating Peptides to Improve Their Efficacy as a Drug Delivery System. *Pharmaceutics*. 14:907. https://doi.org/10.3390/pharmaceutics14050907
14. Zhang Q, Gao H, He Q. (2015) Taming Cell Penetrating Peptides: Never Too Old To Teach Old Dogs New Tricks. *Mol Pharm*. 12:3105-3118. https://doi.org/10.1021/acs.molpharmaceut.5b00428
15. Zhang Q, Liu N, Wang J, et al. (2023) The Recent Advance of Cell-Penetrating and Tumor-Targeting Peptides as Drug Delivery Systems Based on Tumor Microenvironment. *Mol Pharm*. 20:789-809. https://doi.org/10.1021/acs.molpharmaceut.2c00629

16. Todaro B, Ottalagana E, Luin S, Santi M. (2023) Targeting Peptides: The New Generation of Targeted Drug Delivery Systems. *Pharmaceutics*. 15:1648. https://doi.org/10.3390/pharmaceutics15061648
17. Liu R, Li X, Xiao W, Lam KS. (2017) Tumor-targeting peptides from combinatorial libraries. *Adv Drug Deliv Rev.* 110-111:13-37. https://doi.org/10.1016/j.addr.2016.05.009
18. Yang SB, Banik N, Han B, Lee DN, Park J. (2022) Peptide-Based Bioconjugates and Therapeutics for Targeted Anticancer Therapy. *Pharmaceutics*. 14:1378. https://doi.org/10.3390/pharmaceutics14071378
19. Arap MA, Lahdenranta J, Mintz PJ, et al. (2004) Cell surface expression of the stress response chaperone GRP78 enables tumor targeting by circulating ligands. *Cancer Cell*. 6:275-284. https://doi.org/10.1016/j.ccr.2004.08.018
20. Wang SH, Yu J. (2016) Data for peptide-binding assay with oriented immobilization of GRP78 in Biacore. *Data Brief*. 7:1696-1699. https://doi.org/10.1016/j.dib.2016.04.064
21. Wang SH, Lee AC, Chen IJ, et al. (2016) Structure-based optimization of GRP78-binding peptides that enhances efficacy in cancer imaging and therapy. *Biomaterials*. 94:31-44. https://doi.org/10.1016/j.biomaterials.2016.03.050
22. Wang SH, Yu J. (2018) Structure-based design for binding peptides in anti-cancer therapy. *Biomaterials*. 156:1-15. https://doi.org/10.1016/j.biomaterials.2017.11.024
23. Daniel G, Hilan G, Ploeg L, Sabatino D. (2024) Self-assembly of amphiphilic helical-coiled peptide nanofibers and inhibition of fibril formation with curcumin. *Bioorg Med Chem Lett*. 102:129682. https://doi.org/10.1016/j.bmcl.2024.129682
24. Lozada C, Gonzalez S, Agniel R, et al. (2023) Introduction of constrained Trp analogs in RW9 modulates structure and partition in membrane models. *Bioorg Chem*. 139:106731. https://doi.org/10.1016/j.bioorg.2023.106731
25. Alhakamy NA, Dhar P, Berkland CJ. (2016) Charge Type, Charge Spacing, and Hydrophobicity of Arginine-Rich Cell-Penetrating Peptides Dictate Gene Transfection. *Mol Pharm*. 13:1047-1057. https://doi.org/10.1021/acs.molpharmaceut.5b00871
26. Adami RC, Collard WT, Gupta SA, Kwok KY, Bonadio J, Rice KG. (1998) Stability of peptide-condensed plasmid DNA formulations. *J Pharm Sci*. 87:678-683. https://doi.org/10.1021/js9800477
27. Cebrián J, Kadomatsu-Hermosa MJ, Castán A, et al. (2015) Electrophoretic mobility of supercoiled, catenated and knotted DNA molecules. *Nucleic Acids Res*. 43:e24. https://doi.org/10.1093/nar/gku1255
28. Ryu DW, Kim HA, Song H, Kim S, Lee M. (2011) Amphiphilic peptides with arginines and valines for the delivery of plasmid DNA. *J Cell Biochem*. 112:1458-1466. https://doi.org/10.1002/jcb.23064
29. Baoum A, Ovcharenko D, Berkland C. (2012) Calcium condensed cell penetrating peptide complexes offer highly efficient, low toxicity gene silencing. *Int J Pharm*. 427:134-142. https://doi.org/10.1016/j.ijpharm.2011.08.012
30. Cultrara CN, Shah S, Antuono G, et al. (2019) Size Matters: Arginine-Derived Peptides Targeting the PSMA Receptor Can Efficiently Complex but Not Transfect siRNA. *Mol Ther Nucleic Acids*. 18:863-

870. https://doi.org/10.1016/j.omtn.2019.10.013

31. Su L, Sun Z, Qi F, et al. (2022) GRP75-driven, cell-cycle-dependent macropinocytosis of Tat/pDNA-Ca^{2+} nanoparticles underlies distinct gene therapy effect in ovarian cancer. *J Nanobiotechnology*. 20:340. https://doi.org/10.1186/s12951-022-01530-6
32. Khondee S, Baoum A, Siahaan TJ, Berkland C. (2011) Calcium condensed LABL-TAT complexes effectively target gene delivery to ICAM-1 expressing cells. *Mol Pharm*. 8:788-798. https://doi.org/10.1021/mp100393j
33. Kim Y, Lillo AM, Steiniger SC, et al. (2006) Targeting heat shock proteins on cancer cells: selection, characterization, and cell-penetrating properties of a peptidic GRP78 ligand. *Biochemistry*. 45:9434-9444. https://doi.org/10.1021/bi060264j
34. Liu Y, Steiniger SC, Kim Y, Kaufmann GF, Felding-Habermann B, Janda KD. (2007) Mechanistic studies of a peptidic GRP78 ligand for cancer cell-specific drug delivery. *Mol Pharm*. 4:435-447. https://doi.org/10.1021/mp060122j
35. Joseph SC, Blackman BA, Kelly ML, et al. (2014) Synthesis, characterization, and biological activity of poly(arginine)-derived cancer-targeting peptides in HepG2 liver cancer cells. *J Pept Sci*. 20:736-745. https://doi.org/10.1002/psc.2665
36. Ibáñez M, Gariglio P, Chávez P, Santiago R, Wong C, Baeza I. (1996) Spermidine-condensed DNA and cone-shaped lipids improve delivery and expression of exogenous DNA transfer by liposomes. *Biochem Cell Biol*. 74:633-643. https://doi.org/10.1139/o96-068
37. Yang S, Coles DJ, Esposito A, Mitchell DJ, Toth I, Minchin RF. (2009) Cellular uptake of self-assembled cationic peptide-DNA complexes: multifunctional role of the enhancer chloroquine. *J Control Release*. 135:159-165. https://doi.org/10.1016/j.jconrel.2008.12.015
38. Griesenbach U, Wilson KM, Farley R, et al. (2012) Assessment of the nuclear pore dilating agent trans-cyclohexane-1,2-diol in differentiated airway epithelium. *J Gene Med*. 14:491-500. https://doi.org/10.1002/jgm.2643
39. Alhakamy NA, Berkland CJ. (2013) Polyarginine molecular weight determines transfection efficiency of calcium condensed complexes. *Mol Pharm*. 10:1940-1948. https://doi.org/10.1021/mp3007117
40. Wong-Baeza C, Bustos I, Serna M, et al. (2010) Membrane fusion inducers, chloroquine and spermidine increase lipoplex-mediated gene transfection. *Biochem Biophys Res Commun*. 396:549-554. https://doi.org/10.1016/j.bbrc.2010.04.143
41. Moradpour D, Schauer JI, Zurawski VR Jr, Wands JR, Boutin RH. (1996) Efficient gene transfer into mammalian cells with cholesteryl-spermidine. *Biochem Biophys Res Commun*. 221:82-88. https://doi.org/10.1006/bbrc.1996.0549
42. Zhang J, Wang Z, Min J, et al. (2023) Self-Assembly of Peptide-Lipid Nanoparticles for the Efficient Delivery of Nucleic Acids. *Langmuir*. 39:7484-7494. https://doi.org/10.1021/acs.langmuir.3c00834
43. Chappell WH, Lehmann BD, Terrian DM, Abrams SL, Steelman LS, McCubrey JA. (2012) p53 expression controls prostate cancer sensitivity to chemotherapy and the MDM2 inhibitor Nutlin-3. *Cell Cycle*. 11:4579-4588. https://doi.org/10.4161/cc.22852

44. Lane DP. (1992) Cancer. p53, guardian of the genome. *Nature*. 358:15-16. https://doi.org/10.1038/358015a0
45. Muller PA, Vousden KH. (2014) Mutant p53 in cancer: new functions and therapeutic opportunities. *Cancer Cell*. 25:304-317. https://doi.org/10.1016/j.ccr.2014.01.021
46. Yu W, Pirollo KF, Yu B, et al. (2004) Enhanced transfection efficiency of a systemically delivered tumor-targeting immunolipoplex by inclusion of a pH-sensitive histidylated oligolysine peptide. *Nucleic Acids Res*. 32:e48. https://doi.org/10.1093/nar/gnh049
47. Aydin O, Kanarya D, Yilmaz U, Tunç CÜ. (2022) Determination of Optimum Ratio of Cationic Polymers and Small Interfering RNA with Agarose Gel Retardation Assay. *Methods Mol Biol*. 2434:117-128. https://doi.org/10.1007/978-1-0716-2010-6_7

Figures

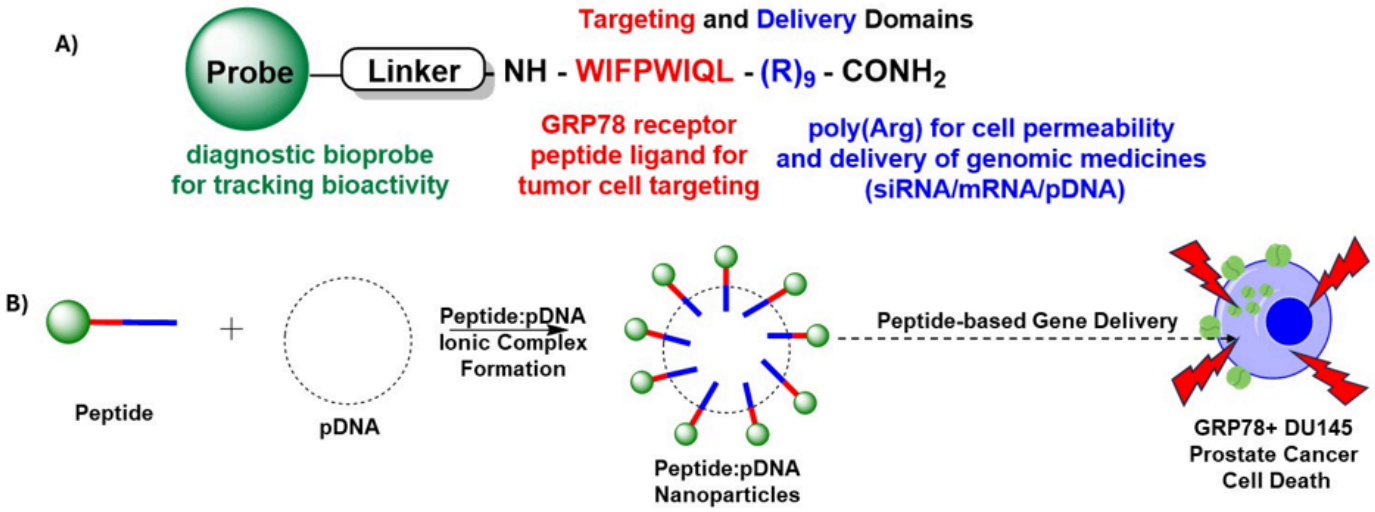

Figure 1

(A) Design of polyarginine-derived GRP78-targeting peptide sequence for (B) gene (pDNA) delivery within the GRP78-overexpressing DU145 prostate cancer cells.

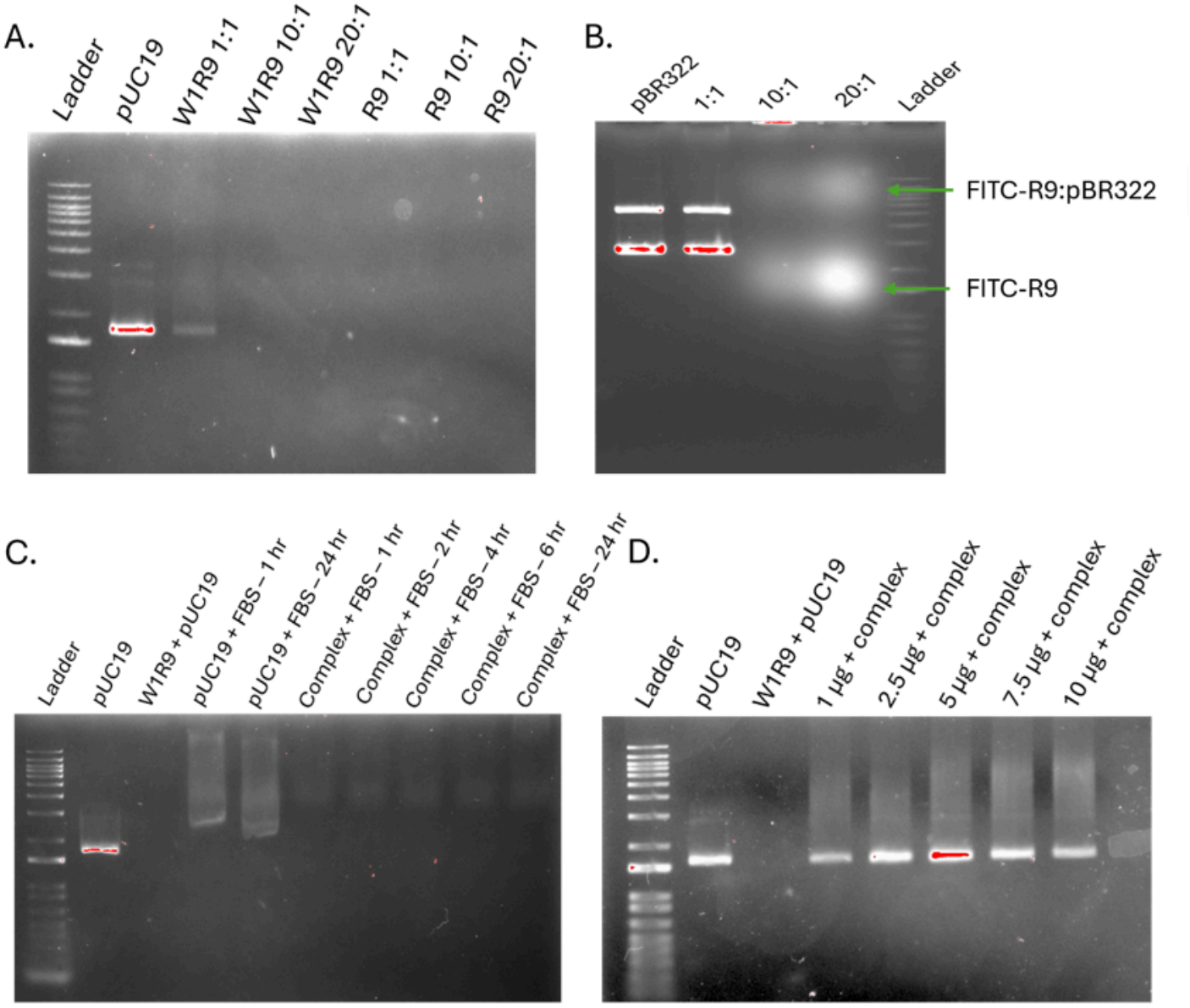

Fig. 2. Agarose (1%) electrophoresis gel shift mobility assays. A. N:P stoichiometric ratios (1-20:1) of peptide (W-R9 and R9) to pUC19, and B. FITC-R9:pBr322 in annealing (50 mM Tris-HCl and 150 mM NaCl, pH 7.5) buffer using ethidium bromide (EtBr) stain. C. A heparin release assay with WR9:pUC19 (10:1 N:P ratio) and various amounts of heparin (1-10 µg) incubated for 30 min. at room temperature in annealing Tris buffer. D. A serum stability assay of WR9:pUC19 (10:1 N:P ratio). Plasmid alone as control. Samples were incubated from 1-24 hours in 10% FBS:EMEM at 37°C.

Figure 2

See image above for figure legend

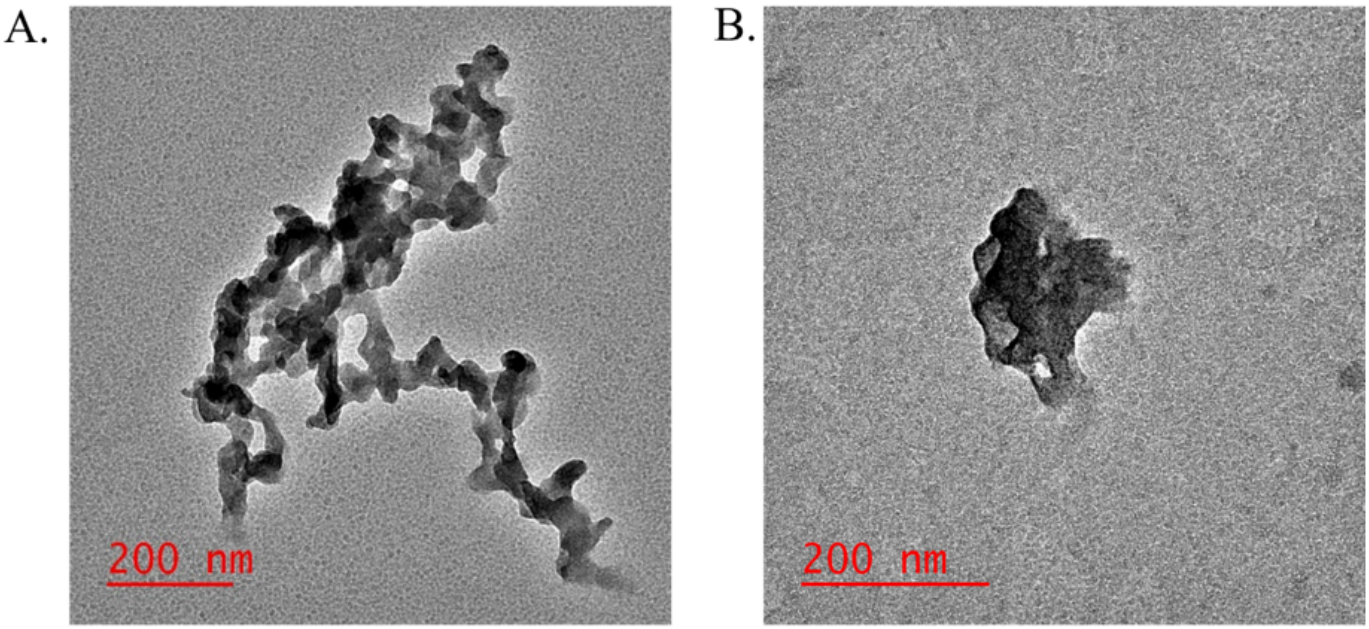

Fig. 3. TEM images of FITC-W-R9 combined with pUC19, A. no $CaCl_2$, and B. 50 mM $CaCl_2$. Samples stained with 1% uranyl acetate in H_2O and dried prior to imaging.

Figure 3

See image above for figure legend

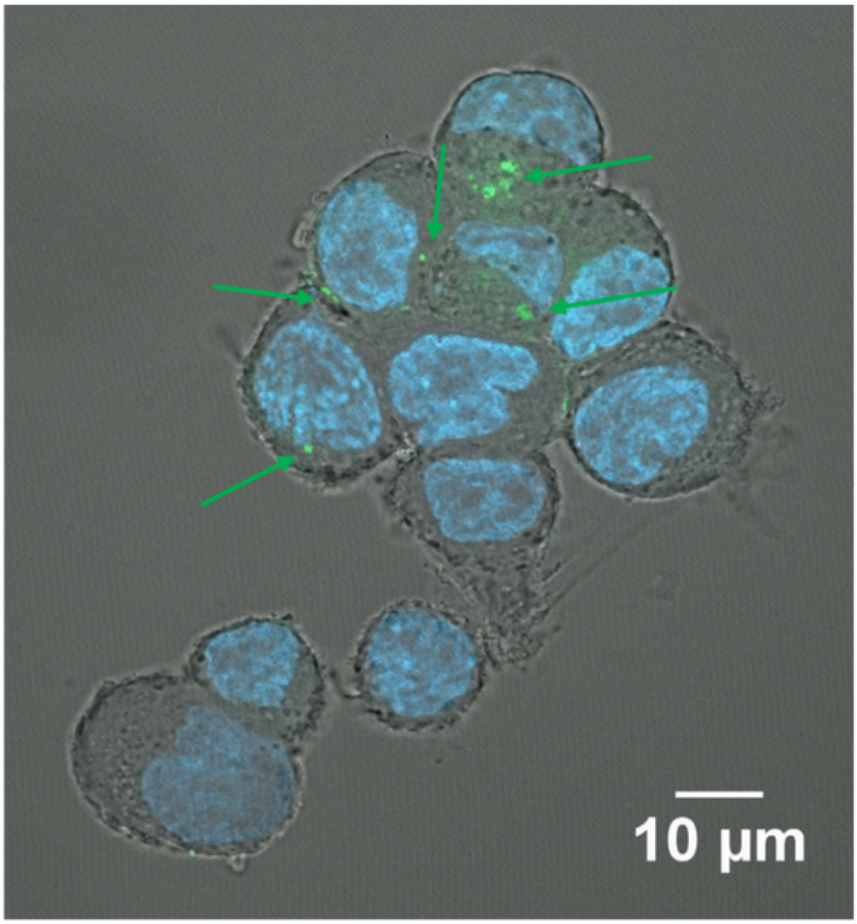

Fig. 4. Confocal fluorescence microscopy imaging of the DU145 cells treated with FITC-labeled peptide FITC-W-R9 in combination with the pBR322 vector at 37˚C in FBS free EMEM for 30 min.

Figure 4

See image above for figure legend

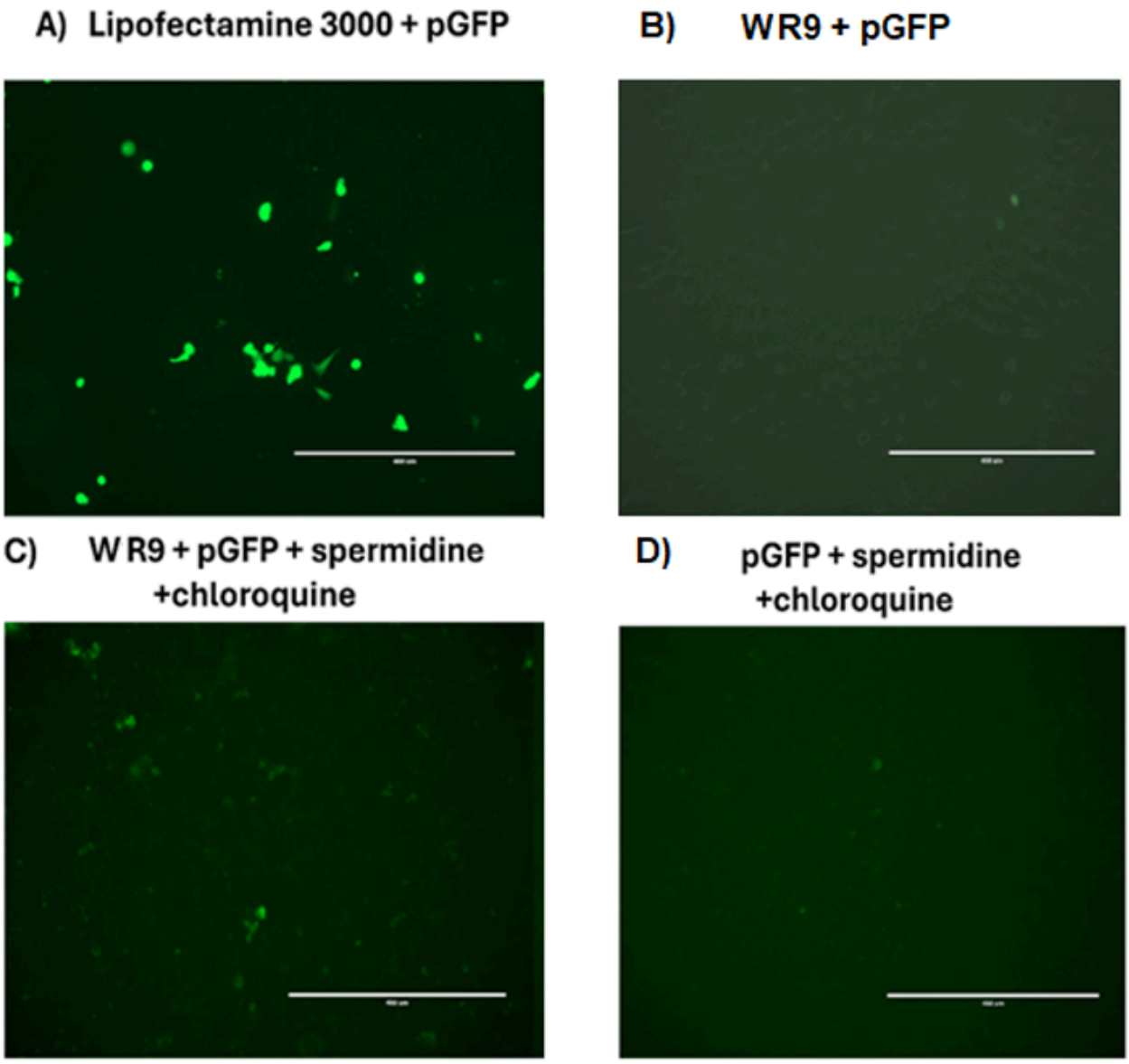

Fig. 5. Optimized transfection conditions using a GFP-expressing plasmid DNA vector. A) Lipofectamine™ 3000 as benchmark pGFP transfection reagent. B) Peptide-based transection (W-R9:pGFP). C) Peptide-based transfection (W-R9:pGFP) with spermidine (17.5 μM) and chloroquine (70 μM) additives. D) pGFP transfection with chloroquine and spermidine, absent of peptide or Lipofectamine™ 3000. Images taken on an EVOS fluorescence microscope using the GFP channel for detection.

Figure 5

See image above for figure legend

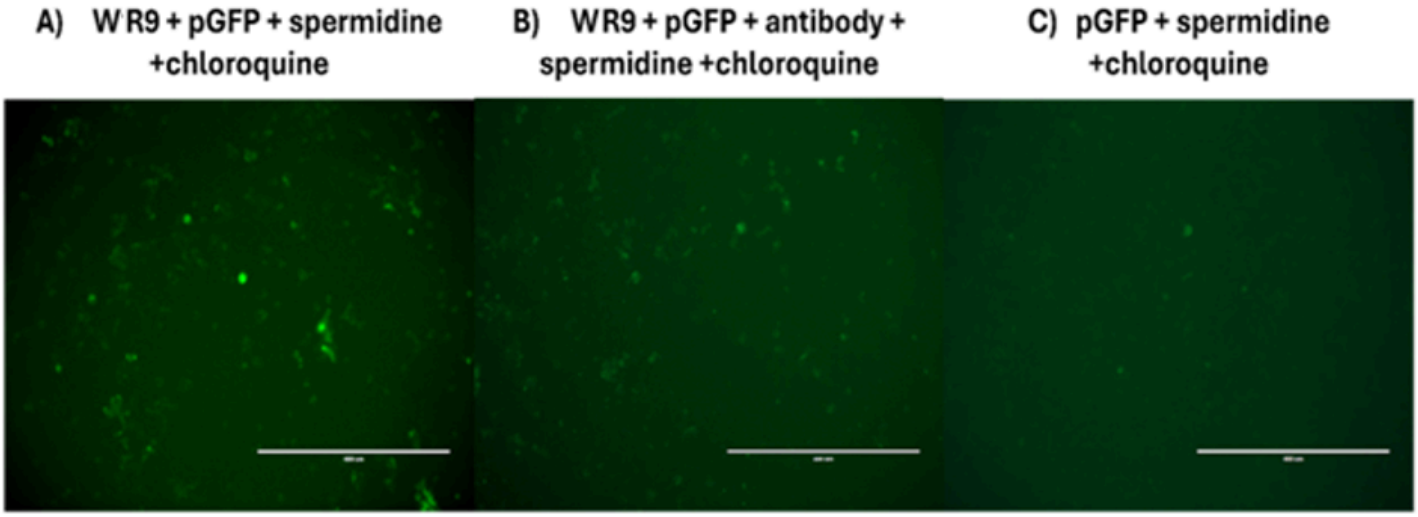

Fig. 6. GRP78-dependent transfection with a GFP-expressing plasmid DNA. The peptide-based (W-R9) pGFP transfection efficiency with spermidine and chloroquine was compared (A) without and (B) with anti-GRP78 (2 µg) treatment. (C) pGFP transfection with spermidine and chloroquine, absent of peptide. Images taken on an EVOS fluorescence microscope using the GFP-channel for detection.

Figure 6

See image above for figure legend

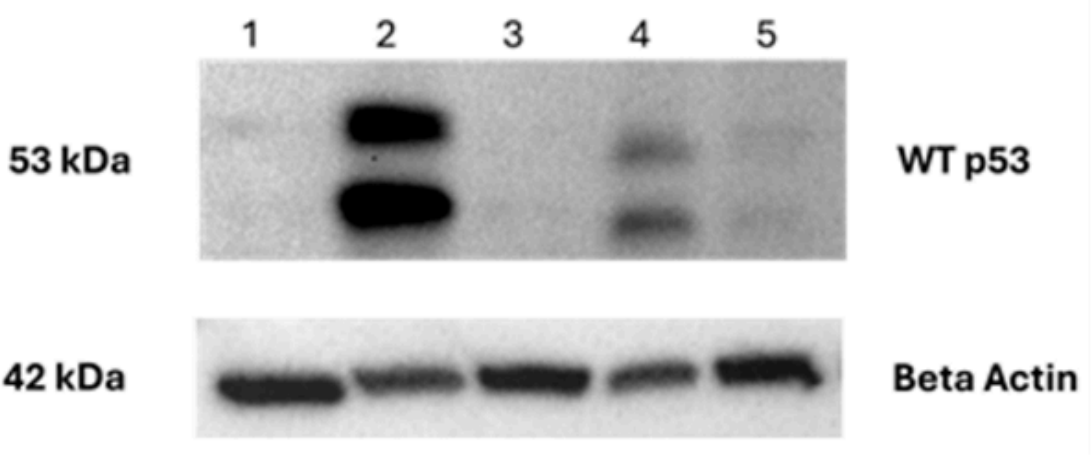

Fig. 7. Transfection of a wild-type p53 pDNA vector. Lane order is as follows: 1) DU145 PCa cells only (control), 2) Lipofectamine™ 3000 + p53 pDNA, 3) FITC-W-R9 + p53 pDNA, 4) FITC-W-R9 + p53 pDNA + chloroquine and spermidine, 5) chloroquine and spermidine + p53 pDNA. Western blot of wild-type (WT) p53, detected with anti-p53 primary antibody. Western blot of beta (β)-actin used as protein loading control.

Figure 7

See image above for figure legend

Supplementary Files

This is a list of supplementary files associated with this preprint. Click to download.

- DanieletalIntJPepResTherBaranySpecialIssueESI.docx